Dynamic Analysis, Stabilization, and Synchronization of an Improved Fractional-Order Chaotic Financial System with External Disturbances

Haojie Yu

***Abstract*—Under the context of current economic environments significantly influenced by external factors, this study constructs a fractional-order financial chaotic system incorporating quadratic external perturbation terms. The system employs new parameter and quadratic term to characterize the nonlinear amplification mechanism of external disturbances. Through rigorous analysis of Lyapunov exponents, attractors, state-space trajectory plots, and equilibrium points, we find that the proposed system exhibits a significantly higher level of dynamic complexity compared to traditional models. For stability control, adaptive sliding mode control is innovatively adopted for asymptotic stabilization analysis of the system's equilibrium points. Through the design of nonlinear sliding manifolds and adaptive control rules, this method flexibly drives the system to converge to equilibrium points. In terms of chaotic synchronization under parameter uncertainties, an adaptive projective synchronization is introduced, which achieves rapid convergence of state errors between the response and master systems. Numerical simulations and theoretical proofs validated all the content presented in this paper.**

***Index Terms*—financial, dynamics, sliding mode control, adaptive projective, stabilization, synchronization**

I. Introduction

CHAOS, as a nonlinear dynamic phenomenon presenting quasi-random behavior in deterministic systems, is particularly complex and challenging in the economic field. This feature is particularly prominent in economic systems, where the inherent instability and complexity of economic operations allow minor external disturbances to be amplified through endogenous feedback mechanisms, potentially triggering systemic turbulences[1-6]. Since the first identification of economic chaos in the 1980s, studies have revealed the intrinsic instability of macroeconomic movements—chaos is essentially an inevitable outcome of nonlinear interactions within economic systems[7-11]. The chaotic characteristics of financial systems are epitomized by extreme sensitivity to external disturbances (the "butterfly effect"), which underscores the urgency of investigating the dynamic behavior and control mechanisms of chaotic systems under perturbations[12]. Traditional integer-order models struggle to accurately describe the complex dynamics of financial markets due to their lack of memory and path-dependency modeling capabilities[13-16]. In contrast, fractional-order chaotic systems have become academic focal points since their inception, owing to their superior ability to characterize high-dimensional complex dynamics[17-21].

Stabilization and synchronization—central to chaos control—remain pivotal research topics in nonlinear dynamics, finding widespread use in fluid mechanics, electrical systems, and biomedicine[22-26]. Current approaches for chaotic system synchronization mainly encompass adaptive regulation, sliding-mode techniques, and drive-response coupling mechanisms, which establish fundamental theoretical support for fractional-order chaotic system regulation[27-30]. However, regarding the stability assessment of financial markets, traditional studies predominantly rely on simple linear or nonlinear control methods, with insufficient applications of adaptive sliding mode control for stabilizing equilibrium points in fractional-order systems[31]. Meanwhile, most synchronization research assumes known system parameters[32-33], whereas parameter uncertainties are pervasive in real-world financial environments, adaptive synchronization approaches become particularly valuable for handling scenarios with indeterminate parameters[34-35]. Chaos control research in the fractional-order framework must not only inherit control theories from integer-order systems but also improve algorithms to address the nonlocality and frequency-dependency characteristics of fractional calculus, thereby coping with the time-varying and complex correlation structures of financial data.

Aiming to bridge the dual gaps in perturbation modeling and control strategies regarding fractional-order financial chaotic systems within existing literature, this paper constructs a novel system with quadratic external perturbation terms. By introducing quadratic terms to characterize the nonlinear amplification mechanism of perturbations and leveraging the high-dimensional representation capabilities of fractional calculus, the model achieves modeling of the financial markets. Regarding control methodologies, adaptive sliding mode control has been innovatively employed for the asymptotic stabilization analysis of system equilibrium points. Through the design of

Manuscript received December 12, 2024; revised Jul 19, 2025.

This work was supported in part by the Key Projects of Science and Technology of Henan Province (242102210190), the Research Subjects of the Private Education Association of Henan Province (HNMXL20241346), and the Education and Teaching Reform Research and Practice Program of Zhengzhou Shengda University (SDJG-2023-YBZ11).

H. J. Yu is an associate professor of Institute of Applied Mathematics, Zhengzhou Shengda University, Zhengzhou, 451191, PR China (e-mail: yuhaojie2009@126.com).

nonlinear sliding surfaces and robust control laws, this approach overcomes the insufficient robustness of traditional methods to parameter perturbations. In addition, an adaptive synchronization algorithm based on projection gain is proposed to cope with the parameter uncertainty in the synchronization process. The real-time estimation of the unknown parameters is used to promote the fast convergence of state error among response system and main system. These findings not only expand the application boundaries of fractional-order chaos theory in finance but also provide new analytical tools for risk management and multi-system coordination in complex economic environments.

This manuscript adopts the following organization: Section II elaborates on the reconstructed fractional-order chaotic financial framework. A dynamical analysis through different comparisons of the system is conducted in Section III. Section IV first applies sliding mode-based control method for asymptotically stabilization of the system. In Section V, an adaptive synchronization controller is formulated to secure the rapid convergence of the error system to zero, even with unknown system parameters. Finally, the research achievements of this article are summarized in Section VI.

II. The New Chaotic Financial System with Quadratic Perturbation

The financial sector's inherent complexity stems from its pronounced sensitivity to external perturbations. For example, government policy decisions, dynamic shifts in market behavior, and domestic or international emergencies can all significantly disrupt financial system stability. In recent years, the increasing frequency and intensity of domestic and global external disturbances have posed profound challenges to financial stability, making systematic research on mitigating their impacts critical for effective risk assessment and resilience enhancement.

Building on extensive numerical experiments with classical financial systems, we introduce a quadratic term and an additional parameter into the system's third equation. The resulting modified system is:

$$\begin{cases} \dot{x}_1 = -rx_1 + x_3 + x_2x_1, \\ \dot{x}_2 = -sx_2 - {x_1}^2 + 1, \\ \dot{x}_3 = -tx_3 - x_1 - mx_1x_2. \end{cases} \tag{1}$$

The quadratic term x_1x_2 in the equation represents the nonlinear coupling between savings volume and price index, characterizing the strong disturbances from current external environment. The newly introduced parameter m serves as a perturbation factor, quantifying the collective impact of additional external influences on economic dynamics.

It is widely recognized that fractional order provides a more realistic description of dynamic systems.

The derivative of Caputo fraction [35]:

$$D_\ell^\partial \Delta = \frac{1}{\Gamma(n-\partial)} \int_{\ell_0}^{\ell} (\ell - \iota)^{n-\partial-1} \Delta^{(n)}(\iota)\, \mathrm{d}\iota, \tag{2}$$

where $n-1 \le \partial < n$.

According to the Caputo definition, the fractional order form of the improved system is:

$$\begin{cases} D_\ell^{q_1} x_1 = -rx_1 + x_3 + x_2x_1, \\ D_\ell^{q_2} x_2 = -sx_2 - {x_1}^2 + 1, \\ D_\ell^{q_3} x_3 = -tx_3 - x_1 - mx_1x_2. \end{cases} \tag{3}$$

Where q_i $(i = 1, 2, 3)$ represents the different derivative order.

III. Dynamic Analysis of the System (3)

In this section, the system is analyzed from the following aspects.

A. Lyapunov Exponents

The dynamic behavior of a three-dimensional chaotic system can be characterized by the positive and negative combinations of its Lyapunov Exponents (LE). In phase space of the system, the positive or negative Lyapunov exponent reflects the stretching or contracting characteristics of the system in different directions, thus determining the chaotic behaviors. In addition, the Lyapunov dimension is a common discriminant. It is a fractal dimension derived from the Lyapunov exponent, serving to measure the dynamical properties of chaotic attractors quantitatively.

The formula for calculating the Lyapunov dimension is:

$$D_L = j + \frac{1}{\left|LE_{j+1}\right|} \sum_{i=1}^{j} LE_i. \tag{4}$$

The impact of parameter m is investigated by the system's dynamic characteristics, Fig. 1 shows the variation curve of the Lyapunov exponent with respect to parameter m.

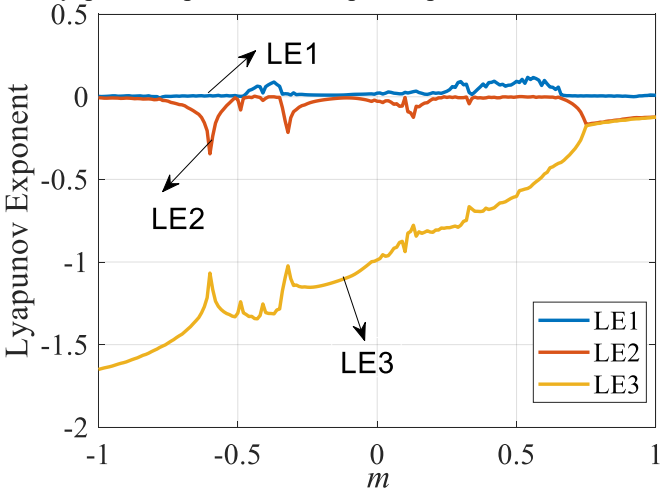

Fig. 1. Lyapunov exponents vs *m*.

Parameter m, as a variable of control, drives the system to evolve along the path of "order → bifurcation → chaos" by changing the positive or negative and magnitude of the exponent. It is a key tool for analyzing the system (3).

In the section, the quantitative analysis of Lyapunov exponents on the dynamic behavior is given. When other parameters $r = 0.9, s = 0.2, t = 1.55$, m takes the values of -0.6, 0.1, 0.5 and 0.8, respectively. Then, the system's chaotic properties are studied through several aspects such as Lyapunov exponent and Lyapunov dimension. Numerical calculations were carried out by MATLAB, and the exact results are shown in Table 1. The curves of the Lyapunov index varying with time are presented respectively in Figs. 2–5.

TABLE I
LYAPUNOV INDEX AND SYSTEM CHARACTERISTICS

m	Lyapunov exponents	Lyapunov dimensions and Dynamic behavior
−0.6	(0, −0.345435, −1.066914), (0, −, −)	$D_L = 2$, Limit loop
0.1	(0.026738, −0.004135, −0.937231), (+, −, −)	$D_L = 2.0241$, Chaos
0.5	(0.104285, 0, −0.602252), (+, 0, −)	$D_L = 2.1732$, Strong chaos
0.8	(0.005489, −0.153947, −0.160393), (+, −, −)	$D_L = 2.003$, Weak chaos

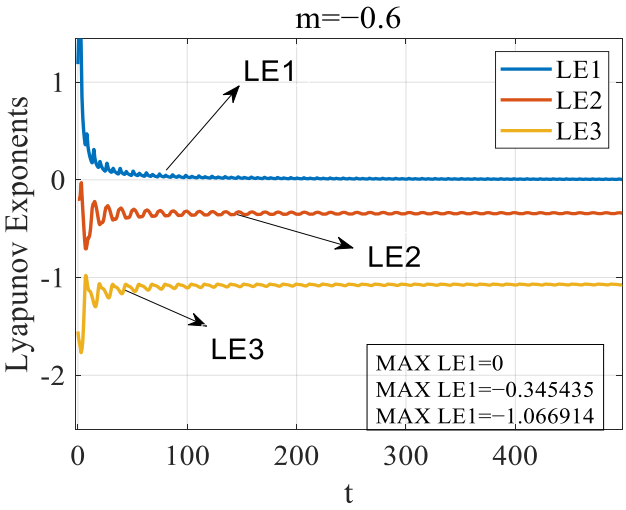

Fig. 2. Lyapunov exponents with m=−0.6.

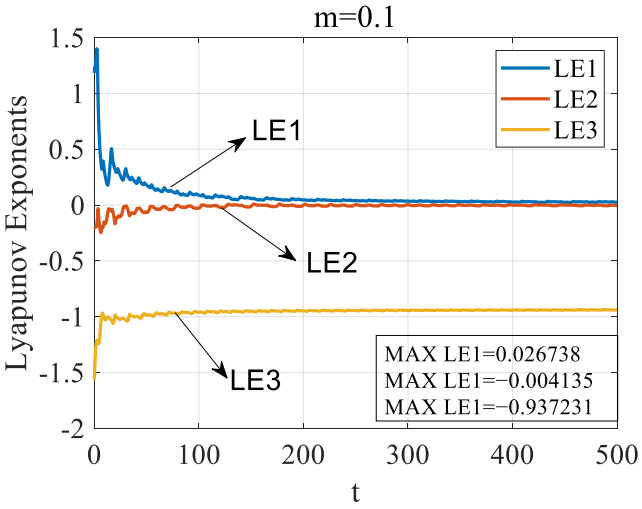

Fig. 3. Lyapunov exponents with m=0.1.

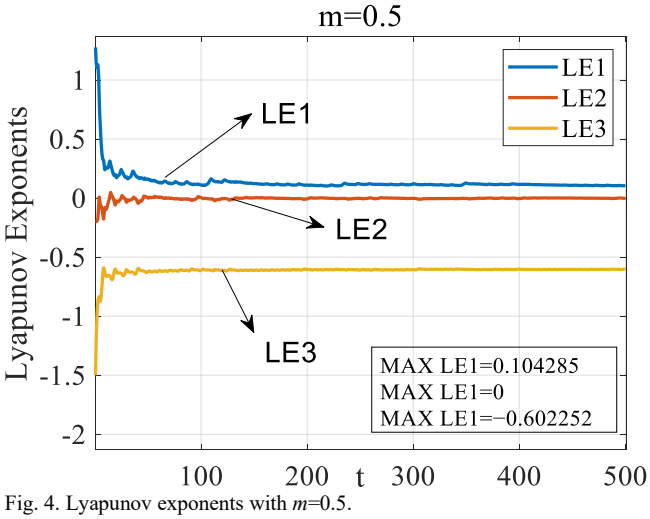

Fig. 4. Lyapunov exponents with m=0.5.

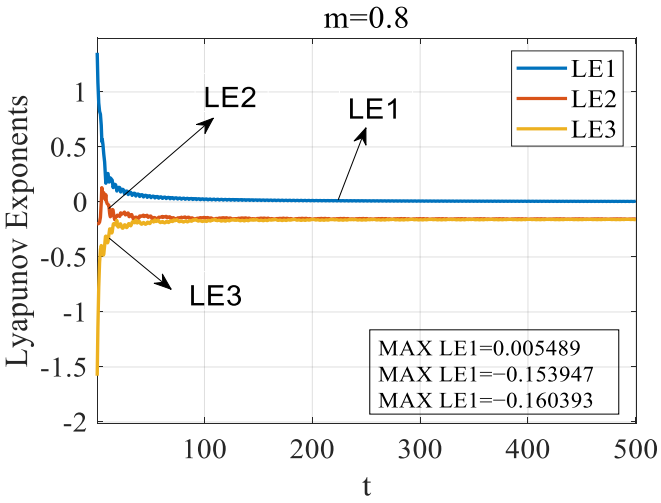

Fig. 5. Lyapunov exponents with m=0.8.

B. Attractors, Phase Portraits, and Power Spectrum Diagrams.

Attractor diagrams intuitively represent the long-term evolutionary trajectories of the system in the phase space. Phase portraits further describe the dynamic relationships between the state variables of system. Power spectrum diagrams (PSD) reveal the frequency components and their intensity distributions of system oscillations through frequency-domain analysis. In order to provide a comprehensive and intuitive description of the dynamic state of the system, this section demonstrates and analyses the dynamic behaviour of the system through these three aspects.

To better investigate the complex dynamic behavior of system (3), we maintain all other initial conditions and parameters constant while varying the parameter m. When $x_1 = 0.01, x_2 = 2.08, x_3 = 0.06$, $q_i = 0.996$, $(i = 1,2,3)$, and $r = 0.9, s = 0.2, t = 1.55$. Figs. 6–15 display the attractor diagrams, phase portraits, and the system's power spectrum diagrams corresponding to distinct parameter values m (i.e., −0.6, 0.1, 0.5, 0.8).

By analyzing the graphs associated with distinct parameter values, the system's dynamical behavior undergoes a sequential evolution: starting from periodicity, transitioning to weak chaos, then strong chaos, and finally reverting to weak chaos. In the periodic stage ($m = -0.6$), the attractor diagram and phase portrait (Fig. 6 trajectory exhibits repetitive periodic characteristics, and the PSD plot (Fig. 7) displays discrete spikes corresponding to the dominant oscillation frequency of the system.

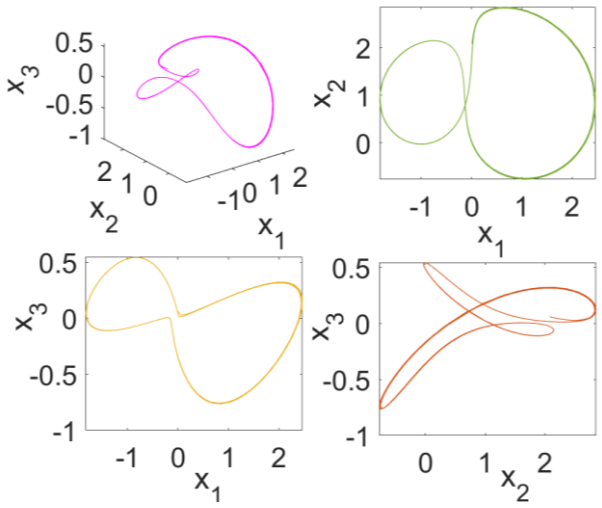

Fig. 6. Phase portraits with m=−0.6.

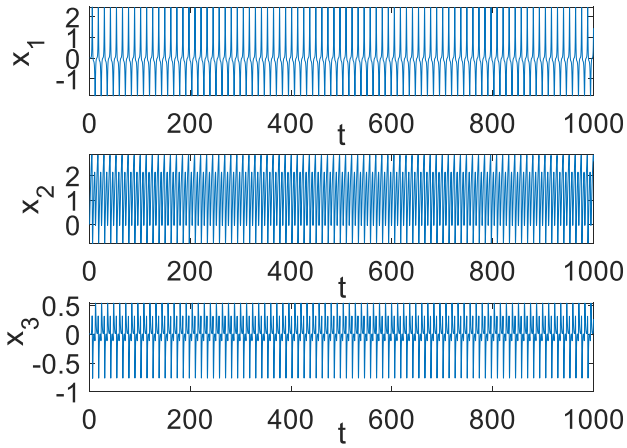

Fig. 7. Power spectrum diagrams with m=−0.6.

When entering the weak chaos stage ($m = 0.1$), the attractor begins to exhibit a fractal structure, the phase portrait trajectory becomes complex and non-repetitive, and continuous background noise appears around the discrete spikes in the PSD plot (Figs. 8–9).

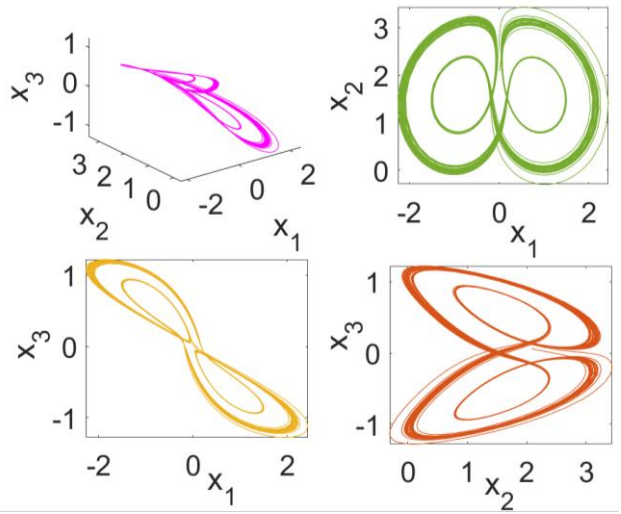

Fig. 8. Phase portraits with m=0.1.

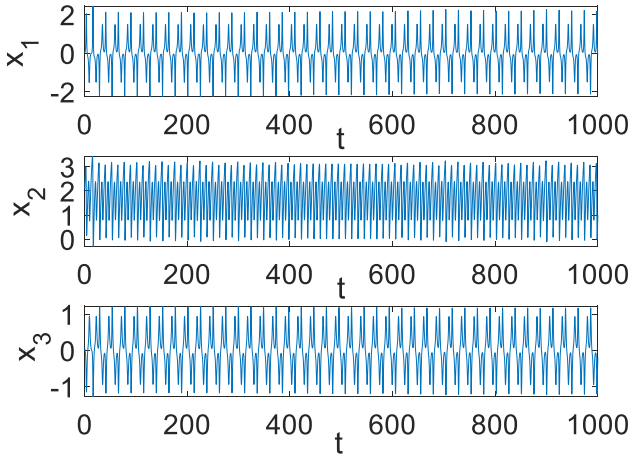

Fig. 9. Power spectrum diagrams with m=0.1.

When $m = 0.5$, the system exhibits strong chaotic behavior, with the attractor forming a typical chaotic structure. The phase portrait trajectory fills the entire phase space region, and the PSD plot shows a continuous broadband spectrum (Figs. 10–11), confirming the presence of broadband components in the system.

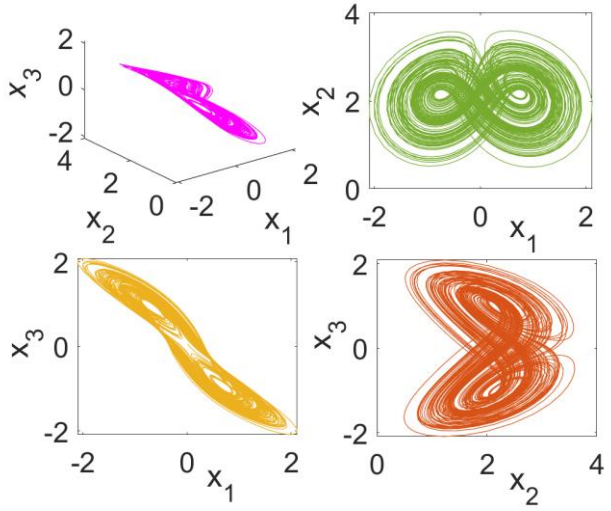

Fig. 10. Phase portraits with m=0.5.

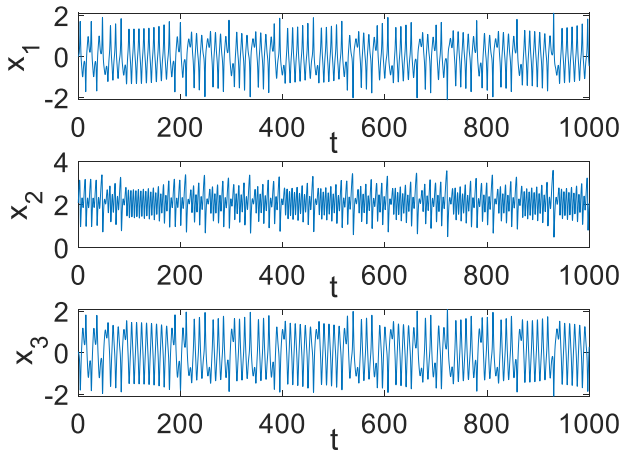

Fig. 11. Power spectrum diagrams with m=0.5.

As parameter $m = 0.8$, system (3) re-enters the stage of weak chaos, with the above characteristics correspondingly weakening, the system's dynamical behavior is shown in Figs. 12–13.

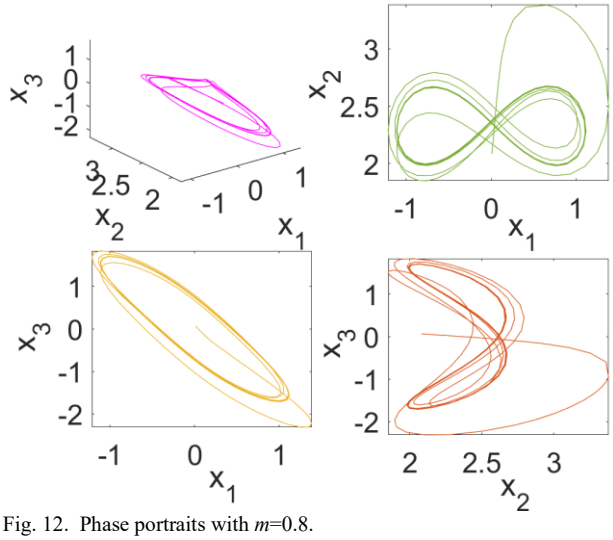

Fig. 12. Phase portraits with m=0.8.

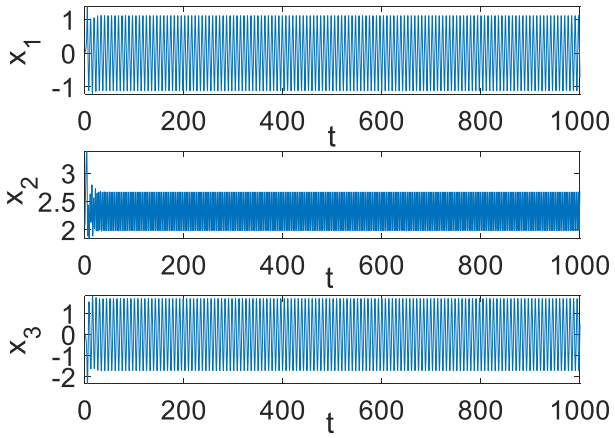

Fig. 13. Power spectrum diagrams with m=0.8.

C. Dynamic Behavior with Different Fractional-Order

The fractional order serves as a critical parameter in fractional-order systems, significantly influencing their dynamical behaviors. In this section, while maintaining fixed starting states $x_1 = 0.01, x_2 = 2.08, x_3 = 0.06,$ parameters $r = 0.9, s = 0.2, t = 1.55, m = 0.5,$ we investigate the potential changes in the system states by varying the fractional order. When $q_1 = 0.95, q_2 = 0.97, q_3 = 0.90,$ the chaotic dynamics exhibited by system (3) are presented in Fig.14 and Fig.15.

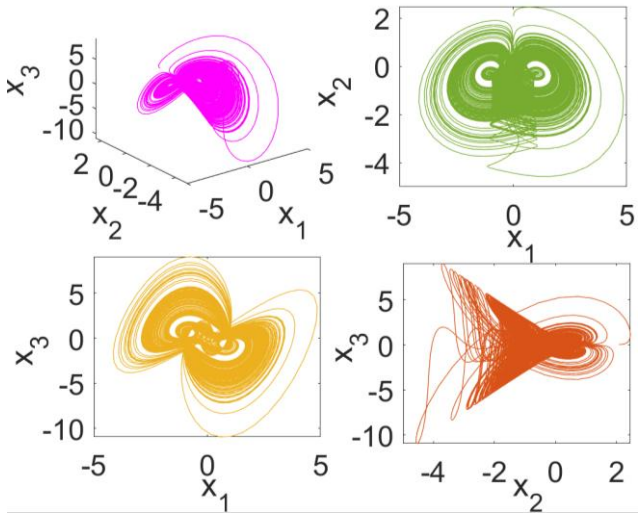

Fig. 14. Phase portraits with $q_1 = 0.95, q_2 = 0.97, q_3 = 0.90$.

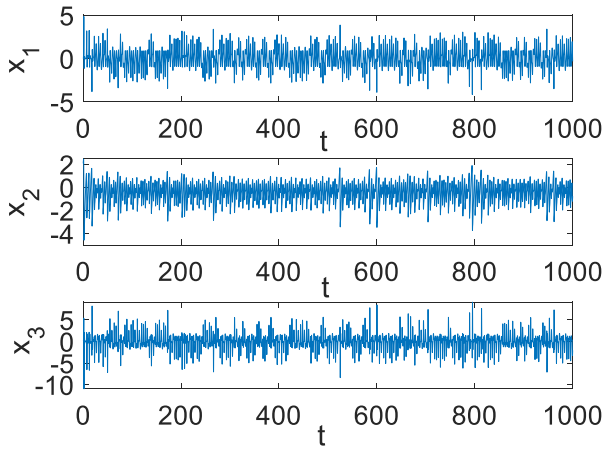

Fig. 15. Power spectrum diagrams with $q_1 = 0.95, q_2 = 0.97, q_3 = 0.90$.

The sensitivity to fractional order can be seen from the Figs. 10–11 and Figs. 14–15. When the fractional order is different, the system's chaotic trajectory grows increasingly complex.

System (3) in fractional order offers a more nuanced framework for analyzing financial dynamics compared to traditional integer-order models. Its ability to generate chaotic behavior under varying derivative orders makes it a valuable tool for simulating market instability, and exploring synchronization phenomena in interconnected economic systems.

D. Dynamic Behavior with Different Initial Conditions

In a chaotic financial system, even slight discrepancies in starting conditions may result in substantial differences in long-term evolutionary trajectories. To explore the system's sensitivity to initial conditions, we conducted numerical simulations by varying initial values. When parameters $r = 0.9, s = 0.2, t = 1.55, m = 0.5,$ the derivative orders $q_1 = 0.95,$ $q_2 = 0.97,$ $q_3 = 0.90,$ initial values $x_1 = 0.05,$ $x_2 = 0.01,$ $x_3 = 0.06.$ The complex chaotic behaviors are shown in Fig.16 and Fig.17.

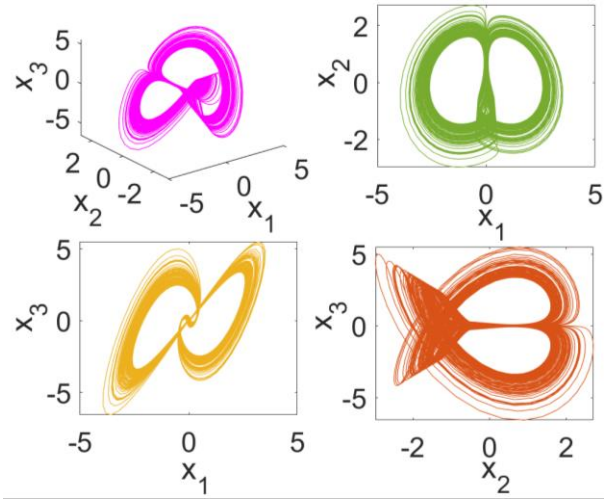

Fig.16. Phase portraits with initial values (0.05,0.01,0.06).

In financial systems, policy intervention can be analogized to modifying the initial values of the system. Meanwhile, the leverage effect inherent in financial systems and investors' psychological biases can amplify the uncertainty of policy outcomes. The uncertainty caused by initial values in chaotic financial systems reflects the limitations of economic

forecasting and the complexity of economic decision-making.

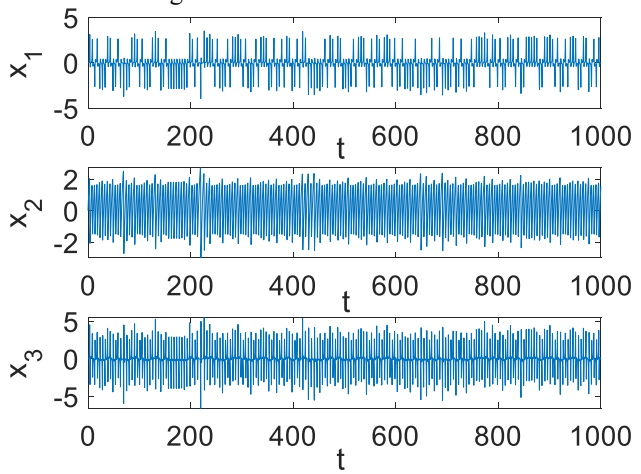

Fig. 17. Power spectrum diagrams with initial values (0.05,0.01,0.06).

E. Equilibrium and Stability

To delve deeper into the complex characteristics of the system (3), an analysis of its equilibrium points is conducted. Solve the following equations:

$$\begin{cases} 0 = -rx_1 + x_3 + x_2x_1, \\ 0 = -sx_2 - x_1^2 + 1, \\ 0 = -tx_3 - x_1 - mx_1x_2. \end{cases} \tag{5}$$

The three equilibrium points of system (3) can be derived, where $P_1 = (0,1/s,0)$, the other equilibrium points P_2, P_3 is solved as follow:

Lemma1. when $\vartheta = \sqrt{(s-t+rst+m)/(m-t)}$, and parameters satisfy $(s-t+rst+m)/(m-t) \geq 0$:

$$P_2 = (\vartheta, \frac{rt+1}{t-m}, \frac{\vartheta(rm+1)}{m-t}),\ P_3 = (-\vartheta, \frac{rt+1}{t-m}, -\frac{\vartheta(rm+1)}{m-t}).$$

Furthermore, for the purpose of examining the equilibrium point's stability, the Jacobian matrix corresponding to system (3) is constructed:

$$\begin{pmatrix} x_2 - r & x_1 & 1 \\ -2x_1 & -s & 0 \\ -1 - mx_2 & -mx_1 & -t \end{pmatrix}. \tag{6}$$

Then the characteristic equations were derived:

$$E(\lambda) = \lambda^3 + \alpha_1\lambda^2 + \alpha_2\lambda + \alpha_3 = 0.$$

Thus, for the first equilibrium point P_1, substituting the parameter values yields the following characteristic equation:

$$\lambda^3 - 2.35\lambda^2 - 3.365\lambda - 0.571 = 0,$$

the characteristic roots are $\lambda_1 = 3.3917$, $\lambda_2 = -0.8417$, $\lambda_3 = -0.2$. λ_1 is a positive real number, and λ_2, λ_3 are negative, so that P_1 is a saddle point with instability.

For the equilibrium point P_2, P_3, substituting the parameters gives the following equation:

$$\lambda^3 + 0.369\lambda^2 + 1.1214\lambda + 1.1420 = 0,$$

and the roots are $\lambda_1 = -0.7872$, $\lambda_2 = 0.2091 + 1.1861i$, $\lambda_3 = 0.2091 - 1.1861i$. The characteristic root λ_1 is a negative real number, λ_2, λ_3 are a pair of conjugate complex numbers, and the real parts which are positive. So that P_2, P_3 are unstable focus.

This analysis highlights the intricate dynamic characteristics exhibited by the chaotic financial system, providing a more profound learning of its stability and equilibrium properties.

IV. Stabilization by Adaptive Sliding Mode Control

Sliding control of fractional dynamical systems is a control method that combines fractional calculus and sliding mode control strategy. This method has significant advantages in dealing with uncertainty and nonlinear problems, while effectively enhancing the response performance and robustness.

When a system takes the form below:

$$D_t^{q_i} X(t) = AX(t) + F(\mathrm{x},t) + \Gamma(\omega(t)) + \Delta(t) + u(t). \tag{7}$$

Where $X(t)$ denotes the state variable, A is the coefficient matrix, $F(\mathrm{x},t)$ represents the nonlinear function, $\Gamma(\omega(t))$ stands for the model uncertainty term, $\Delta(t)$ indicates the exogenous disturbance, and $u(t)$ signifies the term responsible for control.

Definition 1: For the uncertain fractional order system (7), when $t \geq T$, $\|\mathrm{x}(t)\| \equiv 0$, if a constant $T = T(\mathrm{x}(0)) > 0$ exists, and satisfies $\lim_{t \to T} \|\mathrm{x}(t)\| = 0$, the state exhibited by system (7) is capable of converging to zero within a finite period.

For achieving system's stabilization to the equilibrium point by adaptive sliding mode control, the following definition is given for the controlled system:

$$\begin{cases} D_t^{q_1} x_1 = -rx_1 + x_3 + x_2x_1 + \Gamma_1(\omega(t)) + \Delta_1(t) + u_1(t), \\ D_t^{q_2} x_2 = -sx_2 - x_1^2 + 1 + \Gamma_2(\omega(t)) + \Delta_2(t) + u_2(t), \\ D_t^{q_3} x_3 = -tx_3 - x_1 - mx_1x_2 + \Gamma_3(\omega(t)) + \Delta_3(t) + u_3(t). \end{cases} \tag{8}$$

Where $|\Gamma_i(\omega(t))| \leq \ell_i, |\Delta_i(t)| \leq \lambda_i$, $i = 1,2,3$, parameters ℓ_i, λ_i are unknown, and $\ell_i, \lambda_i > 0$.

Let all equilibrium point be denoted as (χ_1, χ_2, χ_3), and define the control error as:

$$\begin{cases} e_1 = x_1 - \chi_1, \\ e_2 = x_2 - \chi_2, \\ e_3 = x_3 - \chi_3. \end{cases} \tag{9}$$

The error system for the fractional controlled system is as follows:

$$\begin{cases} D_t^{q_1} e_1 = e_3 + \chi_3 + (e_2 + \chi_2 - r)(e_1 + \chi_1) \\ \qquad + \Gamma_1(\omega(t)) + \Delta_1(t) + u_1(t), \\ D_t^{q_2} e_2 = 1 - s(e_2 + \chi_2) - (e_1 + \chi_1)^2 \\ \qquad + \Gamma_2(\omega(t)) + \Delta_2(t) + u_2(t), \\ D_t^{q_3} e_3 = -(e_1 + \chi_1) - t(e_3 + \chi_3) - m(e_1 + \chi_1)(e_2 + \chi_2) \\ \qquad + \Gamma_3(\omega(t)) + \Delta_3(t) + u_3(t). \end{cases} \tag{10}$$

Theorem 1: The designed of sliding mode function is:

$$s_i(t) = D_t^{q_i - 1} e_i + \lambda_i \int_0^t e_i(\tau) d\tau, i = 1,2,3. \tag{11}$$

Where $\lambda_i > 0$, and the control law is:

$$\begin{cases} u_1(t) = -(e_3+\chi_3)-(e_2+\chi_2-r)(e_1+\chi_1) \\ \qquad -(\hat{\ell}_1+\hat{\lambda}_1+\kappa_1|s_1|)\mathrm{sign}(s_1), \\ u_2(t) = -1+s(e_2+\chi_2)+(e_1+\chi_1)^2 \\ \qquad -(\hat{\ell}_2+\hat{\lambda}_2+\kappa_2|s_2|)\mathrm{sign}(s_2), \\ u_3(t) = (e_1+\chi_1)+t(e_3+\chi_3)+m(e_1+\chi_1)(e_2+\chi_2) \\ \qquad -(\hat{\ell}_3+\hat{\lambda}_3+\kappa_3|s_3|)\mathrm{sign}(s_3). \end{cases} \tag{12}$$

The adaptive law is given by:

$$\begin{cases} D_t^q\hat{\ell}_i = \mu_i|s_i|, \\ D_t^q\hat{\lambda}_i = \nu_i|s_i|. \end{cases} \tag{13}$$

Where $\hat{\ell}_i, \hat{\lambda}_i$ are the estimated value of ℓ_i, λ_i, μ_i, ν_i, κ_i is the positive real feedback gain of the controller, and the controlled system achieves progressive stability in finite time.

Proof. When moving on the sliding surface, in order for the error system (10) to operate in sliding mode, the conditions below must be met:

$$\begin{cases} s(t) = 0, \\ \dot{s}(t) = 0. \end{cases} \tag{14}$$

Differentiating the sliding mode function yields the following equation:

$$\dot{s}_i(t) = D_t^{q_i}e_i + \lambda_i e_i, i = 1,2,3. \tag{15}$$

Consider the function $\dot{s}(t) = 0$, the dynamics in sliding mode can be generated as:

$$D_t^{q_i}e_i = -\lambda_i e_i, i = 1,2,3. \tag{16}$$

When $e_i(t) \to 0$, based on Definition 1, the system (10) is asymptotically stable on the sliding surface.

When not moving on the sliding surface, Lyapunov function: $V(t) = \sum_{i=1}^{3} V_i$ is constructed, which is a positive-definite function:

$$V_i = \frac{1}{2}s_i^2(t) + \frac{1}{2\mu_i}(\hat{\ell}_i - \ell_i)^2 + \frac{1}{2\nu_i}(\hat{\lambda}_i - \lambda_i)^2,\ i = 1,2,3. \tag{17}$$

Take the derivative of V_i, the results of the calculations are as follows:

$$\begin{aligned} D_t^q V_i &= s_i(t)D_t^q s_i(t) + \frac{1}{\mu_i}(\hat{\ell}_i - \ell_i)D_t^q\hat{\ell}_i + \frac{1}{\nu_i}(\hat{\lambda}_i - d\lambda_i)D_t^q\hat{\lambda}_i \\ &= s_i(t)(D_t^{q_i}e_i + \lambda_i e_i) + \frac{1}{\mu_i}(\hat{\ell}_i - \ell_i)D_t^q\hat{\ell}_i + \frac{1}{\nu_i}(\hat{\lambda}_i - d\lambda_i)D_t^q\hat{\lambda}_i \\ &= s_i(t)(\Gamma_i(\omega(t)) + \Delta_i(t) - (\hat{\ell}_i + \hat{\lambda}_i + \kappa_i|s_i|)\mathrm{sign}(s_i)) \\ &\quad + (\hat{\ell}_i - \ell_i)|s_i| + (\hat{\lambda}_i - \lambda_i)|s_i|. \end{aligned} \tag{18}$$

By the properties of the sign function, we can obtain:

$$\begin{aligned} D_t^q V_i &\le (|\Gamma_i(\omega(t)| + |\Delta_i(t)|)|s_i| - (\hat{\ell}_i + \hat{\lambda}_i + \kappa_i)|s_i| \\ &\quad + (\hat{\ell}_i - \ell_i)|s_i| + (\hat{\lambda}_i - \lambda_i)|s_i| \\ &\le (\ell_i + \lambda_i)|s_i| - (\hat{\ell}_i + \hat{\lambda}_i + \kappa_i)|s_i| \\ &\quad + (\hat{\ell}_i - \ell_i)|s_i| + (\hat{\lambda}_i - \lambda_i)|s_i| \\ &= -\kappa_i|s_i|. \end{aligned} \tag{19}$$

When κ_i are non-negative real number,

$$\dot{V}(t) = \sum_{i=1}^{3}\dot{V}_i \le -\sum_{i=1}^{3}\kappa_i|s_i| < 0. \tag{20}$$

According to the Lyapunov stability theory,

$$s_i(t) \to 0, \tag{21}$$

therefore

$$e_i(t) \to 0, i = 1,2,3, \tag{22}$$

and Theorem 1 thus stands proven.

Numerical Simulation: When the parameter $r = 0.9, s = 0.2, t = 1.55, m = 0.5$, the fractional derivative $q_1 = 0.95, q_2 = 0.97, q_3 = 0.90$, initial value $(x_1, x_2, x_3) = (2.01, 2.08, 2.06)$, the model uncertainty term $\Gamma_i(\omega(t)) = -0.5\sin(t)x_i$, the external disturbance $\Delta_i(t) = 0.5\sin(t)$. At last, select the parameters $\lambda_i = 5$, $\kappa_i = 1.5$, in light of the simulation findings, the controlled error system (10) asymptotic stability at zero, which verifies the validity of the control law (12) and adaptive law (13). The numerical simulation results are presented in Figs. 18–19.

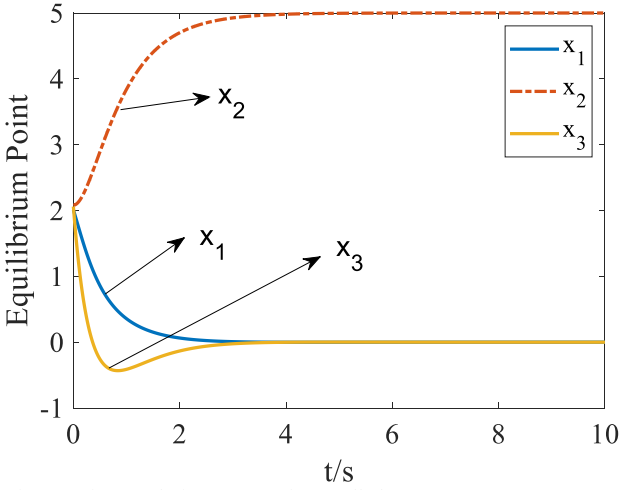

Fig. 18. Time evolution curves of controlled system (8) at P_1.

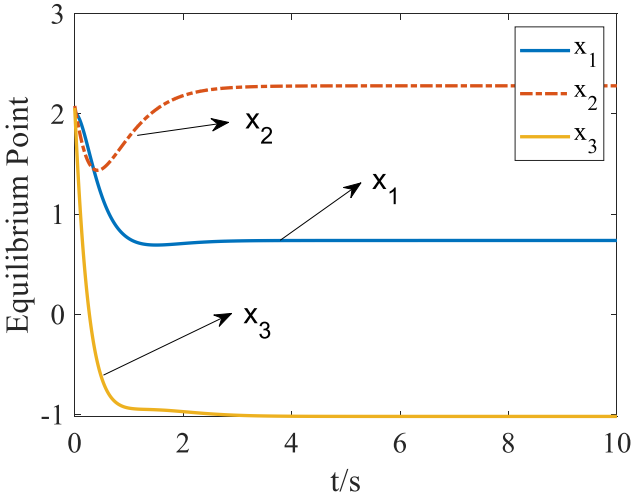

Fig. 19. Time evolution curves of controlled system (8) at $P_{2,3}$.

From the Figs. 18–19, it is evident that each state variable of the system exhibits asymptotic stability. Moreover, the adaptive sliding mode control method is not only applicable to nonlinear control systems but also effective for linear

control systems. This approach provides a practical framework for controlling economic systems, enabling policymakers or managers to implement dynamic interventions effectively. Furthermore, the methodology is highly generalizable and can be readily extended to other complex systems.

V. Synchronization by Adaptive Projective Control

In this section, adaptive projective synchronization is applied to synchronize the new system. The drive system is taken as system (3), with the response system defined as follows:

$$\begin{cases} D_t^{q_1} w_1 = -\alpha w_1 + w_1 w_2 + w_3 + v_1(t), \\ D_t^{q_2} w_2 = -w_1^2 - \beta w_2 + 1 + v_2(t), \\ D_t^{q_3} w_3 = -w_1 - \delta w_3 - \omega w_1 w_2 + v_3(t). \end{cases} \tag{23}$$

Where $\alpha, \beta, \delta, \omega$ is the estimates of unknown parameters r, s, t, m. The estimation errors of the parameters are expressed as:

$$\varepsilon_1 = \alpha - r, \varepsilon_2 = \beta - s, \varepsilon_3 = \omega - m, \varepsilon_4 = \delta - t. \tag{24}$$

The synchronization error is given by:

$$e_1 = w_1 - x_1, e_2 = w_2 - x_2, e_3 = w_3 - x_3. \tag{25}$$

The error system is obtained by subtracting (3) from (23):

$$\begin{cases} D_t^{q_1} e_1 = r x_1 - \alpha w_1 + w_1 w_2 - x_1 x_2 + e_3 + v_1(t), \\ D_t^{q_2} e_2 = x_1^2 - w_1^2 + s x_2 - \beta w_2 + v_2(t), \\ D_t^{q_3} e_3 = -e_1 + m x_1 x_2 - \omega w_1 w_2 + t x_3 - \delta w_3 + v_3(t). \end{cases} \tag{26}$$

The adaptive projective feedback controller is formulated as:

$$\begin{cases} v_1(t) = x_1 x_2 - w_1 w_2 - e_3 - t_1 e_1, \\ v_2(t) = w_1^2 - x_1^2 - t_2 e_2, \\ v_3(t) = e_1 + \omega w_1 w_2 - m x_1 x_2 - t_3 e_3. \end{cases} \tag{27}$$

Where t_1, t_2, t_3 are positive constants. The adaptive update law of the parameter estimates is designed as follows:

$$\begin{cases} D_t^q \alpha = w_1 e_1, \\ D_t^q \beta = w_2 e_2, \\ D_t^q \omega = w_1 w_2 e_3, \\ D_t^q \delta = w_3 e_3. \end{cases} \tag{28}$$

Theorem 2: Under the adaptive projective feedback control unit (27) along with adaptive law of parameters (28), the response system (23) achieves asymptotic synchronization with the drive system (3), this implies that the error system converges to zero.

Proof. Substituting (27) into (26), the error system becomes:

$$\begin{cases} D_t^{q_1} e_1 = -r e_1 - \varepsilon_1 w_1 - t_1 e_1, \\ D_t^{q_2} e_2 = -s e_2 - \varepsilon_2 w_2 - t_2 e_2, \\ D_t^{q_3} e_3 = -t e_3 - \varepsilon_3 w_1 w_2 - \varepsilon_4 w_3 - t_3 e_3. \end{cases} \tag{29}$$

The Lyapunov function is considered:

$$V = \frac{1}{2}\left(\sum_{i=1}^{3} e_i^2 + \sum_{i=1}^{4} \varepsilon_i^2\right). \tag{30}$$

Derivative (30) and substituting (28) and (29), obtain:

$$\begin{aligned} D_t^q V &= e_1 D_t^q e_1 + e_2 D_t^q e_2 + e_3 D_t^q e_3 + \varepsilon_1 D_t^q \varepsilon_1 \\ &\quad + \varepsilon_2 D_t^q \varepsilon_2 + \varepsilon_3 D_t^q \varepsilon_3 + \varepsilon_4 D_t^q \varepsilon_4 \\ &= e_1(-r e_1 - \varepsilon_1 w_1 - t_1 e_1) + e_2(-s e_2 - \varepsilon_2 w_2 - t_2 e_2) \\ &\quad + e_3(-t e_3 - \varepsilon_3 w_1 w_2 - \varepsilon_4 w_3 - t_3 e_3) \\ &\quad + \varepsilon_1 D_t^q(\alpha - r) + \varepsilon_2(\beta - s) \\ &\quad + \varepsilon_3(\omega - m) + \varepsilon_4(\delta - t) \\ &= -r e_1^2 - t_1 e_1^2 - \varepsilon_1 w_1 e_1 - s e_2^2 - t_2 e_2^2 - \varepsilon_2 w_2 e_2 \\ &\quad - t e_3^2 - t_3 e_3^2 - \varepsilon_3 w_1 w_2 e_3 - \varepsilon_4 w_3 e_3 \\ &\quad + \varepsilon_1 D_t^q \alpha + \varepsilon_2 D_t^q \beta + \varepsilon_3 D_t^q \chi + \varepsilon_4 D_t^q \delta \\ &= -r e_1^2 - t_1 e_1^2 - \varepsilon_1 w_1 e_1 - s e_2^2 - t_2 e_2^2 - \varepsilon_2 w_2 e_2 \\ &\quad - t e_3^2 - t_3 e_3^2 - \varepsilon_3 w_1 w_2 e_3 - \varepsilon_4 w_3 e_3 \\ &\quad + \varepsilon_1 w_1 e_1 + \varepsilon_2 w_2 e_2 + \varepsilon_3 w_1 w_2 e_3 + \varepsilon_4 w_3 e_3 \\ &= -r e_1^2 - s e_2^2 - t e_3^2 - t_1 e_1^2 - t_2 e_2^2 - t_3 e_3^2 \\ &< 0. \end{aligned} \tag{31}$$

In accordance with Lyapunov stability theory, asymptotic synchronization between drive system (3) and response system (23) is achieved.

Numerical Simulation: When parameters $r = 0.9, s = 0.2, t = 1.55, m = 0.5$, fractional orders $q_1 = 0.95$, $q_2 = 0.97, q_3 = 0.90$, control coefficients $t_i = 0.5 (i = 1,2,3)$, initial estimates $(\alpha, \beta, \omega, \delta) = (1,2,3,4)$. For the drive system, its initial value is $(x_1, x_2, x_3) = (-1, -2, -1)$. As for the response system, its initial value is designated as $(w_1, w_2, w_3) = (1,2,1)$. The graphical illustration of the data simulation results for the error system (26) is provided in Fig. 20.

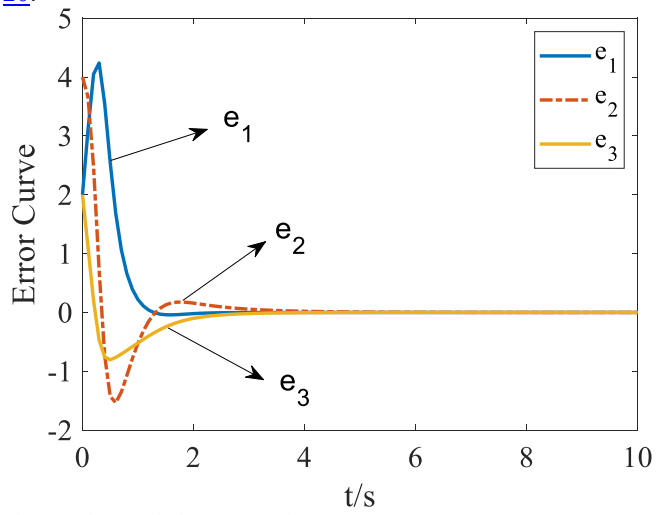

Fig. 20. Time evolution curves of error system (26).

As is readily apparent from the figure, three error states rapidly approach the origin. Thereby validating the effectiveness of the adaptive projective control laws designed in Theorem 2. These results suggest that, under certain conditions, economic systems of different regions or

countries can achieve synchronization.

VI. Conclusions

This study proposes a novel fractional-order chaotic financial system incorporating external disturbances to address the growing complexity of the global economic environment, demonstrating through dynamic analysis, stabilization, and synchronization that it can effectively model real-world financial behaviors like nonlinear interactions and stochastic shocks. The developed adaptive sliding mode control and adaptive projective synchronization methods offer robust solutions for stabilizing unstable equilibria and synchronizing heterogeneous systems with unknown parameters, outperforming other linear approaches. The system's unpredictable evolution paths reflect the volatility of modern financial markets, highlighting the need for adaptive policy-making and accurate market analysis, while its synchronization capability facilitates global economic coordination to enhance financial stability and mitigate systemic risks. Advancing financial modeling and contributing to economic market sustainability, future research will focus on practical implementation in economic systems, integration with machine learning algorithms, and extension to other relevant complex systems for broader applications.

References

[1] G. Liu, X. F. Dou and W. Wang, "Dynamics and nonlinear response of multibody system considering the thermal deformation of clearance joint," *Thermal Science and Engineering Progress*, vol. 64, pp. 103813-103813, 2025.

[2] J. P. Shi, K. He and H. Fang, "Chaos, Hopf bifurcation and control of a fractional-order delay financial system," *Mathematics and Computers in Simulation*, vol. 194, pp. 348-364, 2022.

[3] A. R. Meskine, S. Kaouache and O. O. Aybar, "A new hyperchaotic system with exponential function non linearity: dynamical properties, control hyperchaos and complete synchronization study," *IAENG International Journal of Applied Mathematics*, vol. 54, no. 7, pp. 1329-1335, 2024.

[4] T. F. Lei, B. X. Mao and X. J. Zhou, "Dynamics analysis and synchronous control of fractional-order entanglement symmetrical chaotic systems," *Symmetry*, vol. 13, no. 11, pp. 1996-1996, 2021.

[5] W. J. Wu and Z. Q. Chen, "Hopf bifurcation and intermittent transition to hyperchaos in a novel strong four-dimensional hyperchaotic system," *Nonlinear Dynamics*, vol. 60, pp. 615-630, 2010.

[6] L. Zhang, "Koopman prediction for high-dimensional fractional-order chaotic system with uncertainties," *Communications in Nonlinear Science and Numerical Simulation*, vol. 150, pp. 108965-108965, 2025.

[7] B. Özhan, "Design of a fractional-order neural network-based fixed-time sliding mode controller for chaotic satellite attitude control and synchronization," *Aircraft Engineering and Aerospace Technology*, vol. 97, no. 5, pp. 549–565, 2025.

[8] X. Wang, Z. Wang, and S. Dang, "Dynamic behavior and fixed-time synchronization control of incommensurate fractional-order chaotic system," *Fractal and Fractional*, vol. 9, no. 1, pp. 18-18, 2024.

[9] S. M. Ali, G. Stamov, I. Stamova, et al., "Global asymptotic stability and synchronization of fractional-order reaction–diffusion fuzzy BAM neural networks with distributed delays via hybrid feedback controllers," *Mathematics*, vol. 11, no. 20, pp. 42-48, 2023.

[10] H. Nabil and H. Tayeb, "A fractional-order chaotic Lorenz-based chemical system: Dynamic investigation, complexity analysis, chaos synchronization, and its application to secure communication," *Chinese Physics B*, vol. 33, no. 12, pp. 120503-120503, 2024.

[11] Q. Wang, H. Sang, and P. Wang, "A novel 4D chaotic system coupling with dual-memristors and application in image encryption," *Scientific Reports*, vol. 14, no. 1, pp. 29615-29615, 2024.

[12] X. Feng and J. Gao, "Predefined-time synchronization of fractional-order memristive neural networks with time-varying delay," *IAENG International Journal of Applied Mathematics*, vol. 55, no. 4, pp. 763-767, 2025.

[13] P. Muthukumar and N. Khan, "The large key space image encryption algorithm based on modulus synchronization between real and complex fractional-order dynamical systems," *Multimedia Tools and Applications*, vol. 82, no. 12, pp. 17801–17825, 2023.

[14] S. H. Chen, Q. K. Song, Z. J. Zhao, et al. "Global asymptotic stability of fractional-order complex-valued neural networks with probabilistic time-varying delays." *Neurocomputing*, vol. 450, pp. 311-318, 2021.

[15] P. Gholamin and A. Sheikhani, "Dynamic analysis of a new three-dimensional fractional chaotic system," *Pramana*, vol. 92, no. 11, pp. 1-14, 2019.

[16] D. Cafagna and G. Grassi, "Fractional-order chaos: a novel four-wing attractor in coupled Lorenz systems," *International Journal of Bifurcation and Chaos*, vol. 19, pp. 3329-3338, 2009.

[17] Z. Zhang, J. Zhang and F. Cheng, "Bifurcation analysis and stability criterion for the nonlinear fractional-order three-dimensional financial system with delay," *Asian Journal of Control*, vol. 21, pp. 1-11, 2019.

[18] S. Iqbal and J. Wang, "Analysis of a novel fractional order hyper-chaotic system: Dynamics, stability and synchronization analysis," *Physics Letters A*, vol. 555, pp. 130770-130770, 2025.

[19] Z. Sun, S. Shao and Z. Zhang, "PD sliding mode control of active suspension based on adaptive disturbance observer," *Measurement Science and Technology*, vol. 36, no. 7, pp. 076211-076211, 2025.

[20] I. Javaria, A. Salman, M. Muhammad, R. Ayesha, "Control analysis of virotherapy chaotic system," *Journal of Biological Dynamics*, vol. 16, no. 1, pp. 585-595, 2022.

[21] P. Zhang and Q. Wang, "Dynamics analysis and adaptive synchronization of a class of fractional-order chaotic financial systems," *Fractal and Fractional*, vol. 8, no. 10, pp. 562-562, 2024.

[22] H. Malaikah and F. J. Alabdali, "Analysis of noise on ordinary and fractional-order financial systems," *Fractal and Fractional*, vol. 9, 5, 316-316, 2025.

[23] A. E. Assali and R. Li, "Laplace transform for a new adaptive predefined stability theorem and its application to the synchronization of chaotic systems," *Chaos, Solitons and Fractals: the interdisciplinary journal of Nonlinear Science, and Nonequilibrium and Complex Phenomena*, vol. 199, no. P2, pp. 116778-116778, 2025.

[24] S. Shanmugam, P. Durairaj, R. Vadivel and K. Rajagopal, "Exponential synchronization for Markovian jump Lur'e complex networks using sliding mode control: Application to circuit system," *European Journal of Control*, vol. 85, pp. 101254-101254, 2025.

[25] H. Zhao, Q. Zhao and C. Liu, "Synchronization of Chen's chaotic systems based on single sliding mode controller," *Journal of Physics: Conference Series*, vol. 2921, no. 1, pp. 012017-012017, 2024.

[26] B. Subartini, et al, "Multistability in the finance chaotic system, its bifurcation analysis and global chaos synchronization via integral sliding mode control," *IAENG International Journal of Applied Mathematics*, vol. 51, no. 4, pp. 995-1002, 2021.

[27] X. Wu, H. Zhang, X. Ye and H. Zhang, "Finite-time synchronization of T-S fuzzy memristor-based neural networks subject to algebraic constraints," *Information Sciences*, vol. 719, pp. 122480-122480, 2025.

[28] M. Zhu, D. Gong and Y. Zhao, "Compliant Force Control for Robots: A Survey," *Mathematics*, vol. 13, no. 13, pp. 2204-2204, 2025.

[29] Y. Wang, S. Zhai, M. Du, and P. Zhao, "Dynamic Behaviour of Multi-Stage Epidemic Model with Imperfect Vaccine," *IAENG International Journal of Applied Mathematics*, vol. 52, no.4, pp1052-1060, 2022.

[30] K. Sanjay and K. Praveen, "Analysis and chaos control and synchronization of the nonlinear Newton–Leipnik system via feedback adaptive control techniques," *Journal of Uncertain Systems*, vol. 16, no. 04, pp. 2330002-2330002, 2023.

[31] P. V. L. Em, "Synchronous controller for identical synchronization in networks with arbitrary topological structure of n reaction-diffusion systems of the Hindmarsh-Rose 3D type," *Engineering Letters*, vol. 33, no. 4, pp. 981-997, 2025.

[32] Y. G. Sun, Y. H. Liu, and L. Liu, "Fixed-time adaptive synchronization of fractional-order memristive fuzzy neural networks with time-varying leakage and transmission delays," *Fractal and Fractional*, vol. 9, no. 4, pp. 241-241, 2025.

[33] Z. Ding, J. Wang, S. Li, et al., "Fixed-time synchronization of fractional-order complex-valued delayed neural networks with discontinuous activation functions," *Neural Computing and Applications*, vol. 36, no. 26, pp. 15947–15959, 2024.

[34] Z. Wu and X. Nie, "Finite-time synchronization of fractional-order quaternion-valued delayed Cohen-Grossberg neural networks," *Neural Processing Letters*, vol. 55, no. 9, pp. 12255–12271, 2023.

[35] A. Ricardo, et al, "Stability of gene regulatory networks modeled by generalized proportional Caputo fractional differential equations," *Entropy*, vol. 24, no. 3, pp. 372-372, 2022.